Workspace Analysis in the Design Parameter Space of a 2-DOF Spherical Parallel Mechanism for a Prescribed Workspace: Application to the Otologic Surgery

Damien Chablat, Guillaume Michel, Philippe Bordure, Swaminath Venkateswaran, Ranjan Jha

Workspace Analysis in the Design Parameter Space of a 2-DOF Spherical Parallel Mechanism for a Prescribed Workspace: Application to the Otologic Surgery

Damien Chablat[a,*], Guillaume Michel[b], Philippe Bordure[b], Swaminath Venkateswaran[a], Ranjan Jha[c]

[a] *Laboratoire des Sciences du Numérique de Nantes, UMR CNRS 6004, Nantes, France.*
[b] *CHU de Nantes, 1, place A. Ricordeau, 44093 Nantes, France.*
[c] *BioMedical Instrumentation Division, CSIR- Central Scientific Instruments Organisation, Chandigarh, India.*

Abstract

During Otologic surgery, and more broadly during microsurgery, the surgeon encounters several difficulties due to the confined spaces and micro-manipulations. The purpose of the paper is to design a robot with a prescribed regular workspace shape to handle an endoscope to assist the Otologic surgery. A spherical parallel mechanism with two degrees of freedom is analysed in its design parameter space. This mechanism is composed of three legs (2USP-U) to connect the base to a moving platform connected to a double parallelogram to create a remote center of motion (RCM). Its kinematic properties, i.e. the singularity locus and the number of direct kinematic solutions, are investigated. For some design parameters, non-singular assembly modes changing trajectories may exist and have to be investigated inside the prescribed regular workspace shape. Two sets of design parameters are presented with their advantages and disadvantages.

Keywords: Spherical Mechanism, Otologic Surgery, Cusp points, Parallel robot, Singularities

Highlights

- Design of mechanism for Otologic Surgery;
- Kinematic structure of the proposed mechanism;
- Workspace and Joint space analysis of the proposed 2-DOF Spherical mechanism;
- Influence of the design parameter on the workspace properties;
- Workspace without non-singular assembly modes changing trajectories.

*Corresponding author
Email addresses: Damien.Chablat@cnrs.fr (Damien Chablat), Guillaume.Michel@chu-nantes.fr (Guillaume Michel), Philippe.Bordure@chu-nantes.fr (Philippe Bordure), swaminath.venkateswaran@ls2n.fr (Swaminath Venkateswaran), Ranjan.Jha@csio.res.in (Ranjan Jha)

Nomenclature

$SIROPA$	$Library\ for\ manipulator\ singularities\ analysis$
CAD	$Cylindrical\ Algebraic\ Decomposition$
IKP	$Inverse\ Kinematic\ problem$
DKP	$Direct\ Kinematic\ problem$
det	$Determinant\ of\ Jacobian\ matrix$
R	$Revolute\ Joint$
P	$Prismatic\ Joint$
S	$Spherical\ Joint$
ρ	$Actuated\ Joint\ Variables$
X	$Pose\ Variables$
$\mathbf{A}$	$Direct\ parallel\ Jacobian\ matrices$
$\mathbf{B}$	$Inverse\ serial\ Jacobian\ matrices$
S_α	$\sin(\alpha)$
S_β	$\sin(\beta)$
C_α	$\cos(\alpha)$
C_β	$\cos(\beta)$

1. Introduction

Traditionally, the ear surgeries are performed under binocular Loupes, which allows the surgeon to use both hands during the surgery. Presently, the development of Otologic surgery by endoscopy allows a better view of areas difficult to access [1, 2]. However, the use of an endoscope restricts the surgeon to use both the hands while doing surgery. Therefore, there is a strong expectation on the part of the otologic surgeon for a robotic assist system to perform the surgery comfortably.

There are many advantages for using an endoscope instead of the conventional microscope in otologic surgery. Some of them include a better view with easy access to the operation area and proximity to the patient during the operation. Endoscopic surgeries result in less bone sacrifice and thus improve the patient's recovery period. Despite the many advantages, endoscopic surgeries pose different challenges for the surgeon. Currently, the surgeon can only use one tool at a time in endoscopic surgery, as opposed to two tools with the use of a microscope, as shown in Figure 1. This makes endoscopic surgeries cumbersome because the surgeon must switch from one tool to the other to operate and manage bleeding in the ear. At the time of patient set-up, several factors can change the anatomical position of the head and thus the workspace in which the robot must operate. This leads to changes in the robot's approach angle. It must be able to compensate for this by working amplitudes that are greater than the working space inside the ear alone.

This paper is organized as follows. The first part comprises of the application of robot for the otologic surgery in order to determine the required workspace. A two DOF RCM spherical mechanism is proposed in the second part with detailed kinematic equations. The third part reports the singularity and workspace analysis of the proposed robot in the design parameter space with two case studies to fulfil the design requirements. In the later parts, discussions and conclusions are presented.

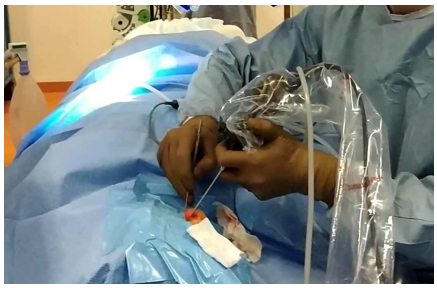

(a) The use of single hand to hold endoscope limits the number of instruments

(b) The surgeon can use two instruments while using a microscope

Figure 1: The comparison of the number of instruments possible to use simultaneously while using an endoscope and a microscope (Dr. Guillaume Michel, CHU Nantes).

2. Application of Robotics for otologic surgery

2.1. Robotics for otologic surgery

Currently, several robotic systems are developed [3], reflecting the interest for robotic assistance in microscopic surgery. In the context of designing a robot to assist the surgeon in otologic surgery, a spherical robot with a parallel structure associated with a double parallelogram was developed [4]. This robot can handle an endoscope to increase the efficiency of the surgeon when compared to the classical binocular performed surgery. The parallel structure should increase the rigidity compared to the existing solution [5]. Many spherical mechanisms exist [6, 7, 8, 9, 10]. They can be divided into two main families (i) those with a virtual center of rotation and (ii) those constrained by a spherical joint or a universal joint (three or two DOF). To form a remote center of motion (RCM), one solution is to use a universal joint associated with two parallelograms. Actuation can be done with prismatic or revolute actuators. The advantage of prismatic actuators is that there is only one solution to the inverse geometric model or one working mode [11, 12]. In order to give the surgeon more mobility, it is necessary to have the largest working space without singularity. By adding an offset in the classical design, we are able to increase this workspace but the properties of the robot change [13]. In [13] the parameter h is added between the universal joint and the mobile platform but the offset on the both legs are removed.

For most parallel or serial manipulators, pose variables and joints variables are linked by algebraic equations and form a so called algebraic variety (sometimes after a straight forward change of variables). The two-kinematic problems (the direct kinematic problem (DKP) and the inverse kinematic problem (IKP)) consist in studying the pre-image of the projection of this algebraic variety onto a subset of unknowns. Solving the DKP remains to computing the possible poses for a given set of joint variables values while solving the IKP remains

to computing the possible joints variables values for a given pose. Algebraic methods have been deeply used in several situations for studying parallel and serial mechanisms, but finally their use is quite confidential in the design process. The number of aspects changes and the number of solutions to the DKP increases. This means that the presence of cusp points or the uniqueness domains in the workspace must be investigated [14]. In this paper we will present the mechanism properties for a given offset that allow non-singular assembly mode changing trajectories [15]. The SIROPA library written in Maple will be used to compute the singularity equations using Groebner bases, do the cylindrical algebraic decomposition (CAD) as well as the trajectories [16, 17]. The paper presents the design of a robotic system, which assist the surgeon in visualizing the inner part of the ear while performing surgery using an endoscope. This would facilitate the use of the endoscope in microsurgery or even replace any use of the operating microscope. The study of workspace, joint space and singularities together assists the engineers and researchers in the efficient task planning and the selection of the particular configuration of the manipulator for a desired task.

In this paper we will present the mechanism properties for a given offset that allow non-singular assembly mode changing trajectories [15]. The SIROPA library written in Maple will be used to compute the singularity equations using Groebner bases, do the cylindrical algebraic decomposition (CAD) as well as the trajectories [16, 17]. The paper presents the design of a robotic system, which assist the surgeon in visualizing the inner part of the ear while performing surgery using an endoscope. This would facilitate the use of the endoscope in microsurgery or even replace any use of the operating microscope. The study of workspace, joint space and singularities together assists the engineers and researchers in the efficient task planning and the selection of the particular configuration of the manipulator for a desired task.

2.2. Specifications for the otological surgeries

Figure 2 shows the ear in two orientations. The optimal position, for most of the otological surgeries, is when the mastoid is horizontal. Unfortunately, the patient's anatomy does not always allow the ear to be in this position. In the figure on the right, the axis of the ear can therefore be tilted by about 54°. Mobility inside the ear has been studied in [18] with a scan analysis on a population of variable age and sex (n=16, patients from 2 to 79 years old). It can be hypothesized that the center of rotation of the endoscope will be placed in the middle of the ear canal as shown in Figure 3.

In this study, we can isolate the dimensional parameters giving maximum angular variation. Figure 4 represents these variations with a zero diameter for the endoscope in the centre and on the right and left for an endoscope of 3 and 4 mm diameter where the tilt angles are equal to $\pm 13°$ and $\pm 11°$. To ensure that the robot can be used for all patients as well as having the necessary mobility for all ears. Figure 5(left) depicts the nominal cone and its inclination of 54° to reach the most inclined position of Figure 3. The total angle becomes 67°. However we must slightly increase this value because we will define the limit of the workspace by the singularities, where the robot behavior will be less accurate. We choose to search for a tilt angle close to 75°. Workspace can be defined using azimuth, tilt and torsion representation [19] where azimuth angle is [0...360°], tilt angle is [0...75°] and no torsion. For the studied mechanism, we

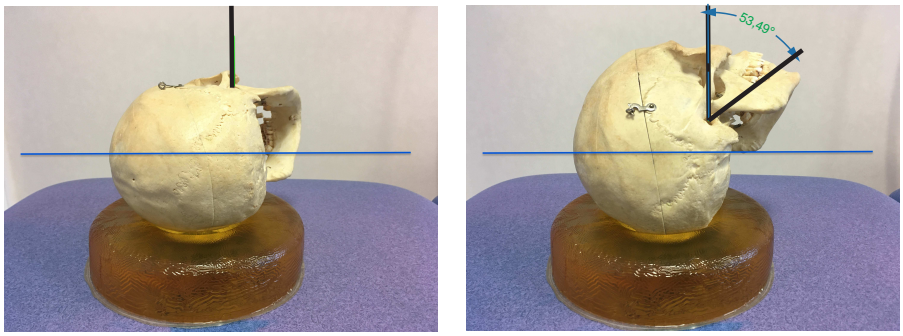

Figure 2: Placement of the ear in relation to the operating table in the optimal (right) and unfavourable (left) position

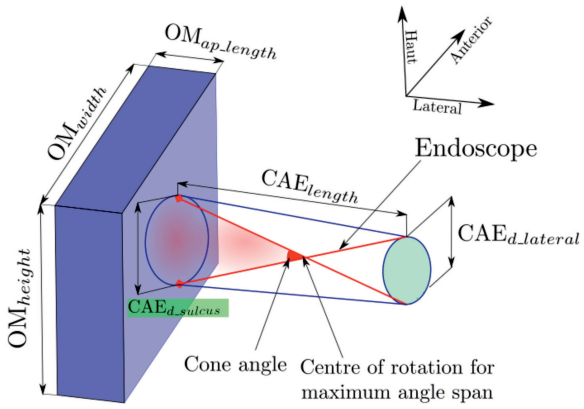

Figure 3: Schematic workspace of the external (cylinder) and middle ear

will use a universal joint based on two orthogonal revolute joints α and β. Figure 5(right) depicts in red the image of the regular workspace shape [20] requested to have the tilt motion in the Euler coordinates. It is possible to include this space either by a square defined by $\alpha = \beta = [-75°...75°]$ or a centered circle with a radius equal to 75°.

Another constraint is to limit the possible interference between the mechanism and the surgeon. Therefore, we can offset the center of rotation by using a RCM made by parallelograms.

3. A remote center of motion mechanism to carry an endoscope

Figure 6 shows an RCM mechanism carrying an endoscope for operations in the ears made by coupling two DOF spherical mechanism with double parallelograms. This mechanism is coupled to a translation mechanism for positioning in the middle ear centre. Another mechanism, not shown in the figure, allows translation of the endoscope for insertion, cleaning and ejection in case the

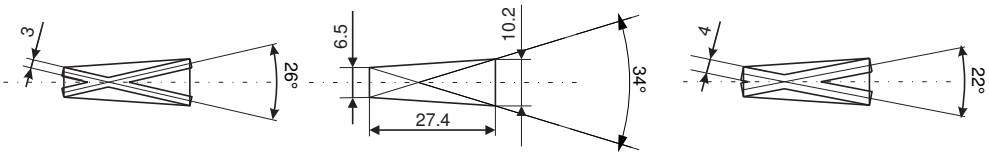

Figure 4: Mobility of the endoscope inside the middle ear

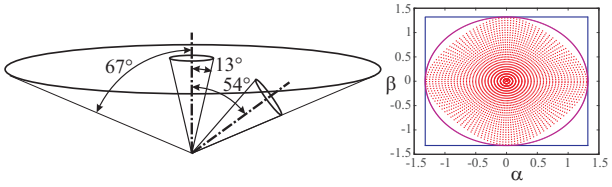

Figure 5: Prescribed regular workspace shape for Otologic surgery

patient wakes up (patent pending) [21]. The spherical parallel mechanism is composed of three limbs and one moving platform. The two first legs, UPS, are composed of a universal joint, a prismatic joint and a spherical joint and the last one is made by a single universal joint and constrains its mobility. The two prismatic joints are actuated. The double parallelogram is attached to the two axes of this joint. Usually, the end points of the UPS legs are in the same plane as the axes of rotation of the universal joint.

In order to obtain the desired workspace, it is possible to vary several design parameters. In this study, one parameter is normalized, the structure remains symmetrical and three length parameters are varied.

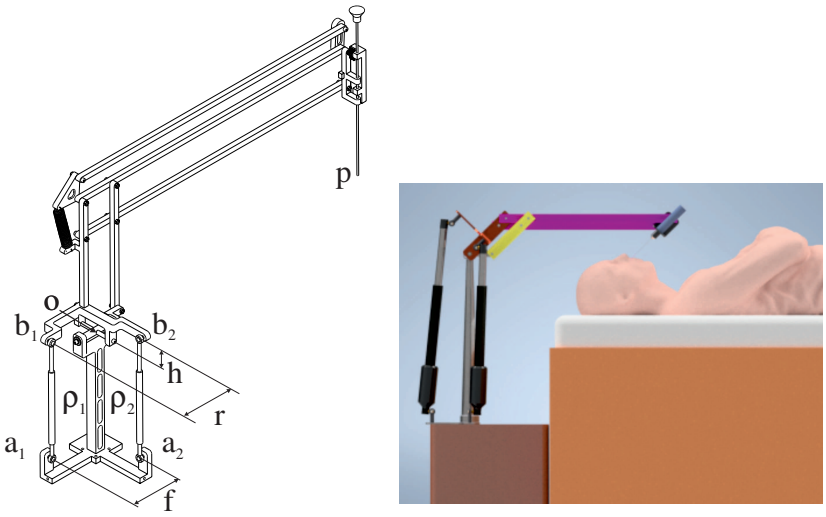

Figure 6: RCM Mechanism with spherical parallel mechanism in its home pose and its location close to the patient

3.1. Kinematic equations

Let $\mathbf{a}_1$ and $\mathbf{a}_2$ be attached to the base, O the center of the universal joint and $\mathbf{b}_1$ and $\mathbf{b}_2$ be attached to the mobile platform in the moving reference frame.

The coordinates are given by

$$\mathbf{o} = [0,0,0]\,, \mathbf{a}_1 = [f,0,-1]^T\,, \mathbf{a}_2 = [0,f,-1]^T\,, \mathbf{b}_1 = [r,0,h]^T\,, \mathbf{b}_2 = [0,r,h]^T \tag{1}$$

The orientation space of the moving platform is fully represented with the variables (α, β). The rotation matrix $\mathbf{R}$ from the base frame to the moving frame is expressed as follows:

$$\mathbf{R} = \mathbf{R}_\alpha \mathbf{R}_\beta = \begin{bmatrix} C_\beta & 0 & S_\beta \\ S_\alpha S_\beta & C_\alpha & -S_\alpha C_\beta \\ -C_\alpha S_\beta & S_\alpha & C_\alpha C_\beta \end{bmatrix} \tag{2}$$

The orientation angles are defined in such a way that $\alpha = \beta = 0$, which represents the "home" pose as depicted in Figure 6. The coordinates of $\mathbf{b}_1$ and $\mathbf{b}_2$ can be written in the base frame as

$$\mathbf{c}_1 = \mathbf{R}\mathbf{b_1} \quad \mathbf{c}_2 = \mathbf{R}\mathbf{b_2} \tag{3}$$

The distance constraints from the two prismatic joints yields

$$||\mathbf{a}_i\mathbf{c}_i|| = \rho_i \quad \text{with} \quad i = 1,2 \tag{4}$$

This leads to the two constraint equations:

$$-2(fh + C_\alpha r)S_\beta + 2(hC_\alpha - fr)C_\beta + f^2 + h^2 + r^2 + 1 = \rho_1^2 \tag{5}$$

$$2h(fS_\alpha + C_\alpha)C_\beta - 2fC_\alpha r + f^2 + h^2 + r^2 + 2S_\alpha r + 1 = \rho_2^2 \tag{6}$$

4. Singularity and workspace analysis

The singularity analysis is done by differentiating the two constraint equations with respect to time that leads the velocity model:

$$\mathbf{A}\omega + \mathbf{B}\dot{\rho} = 0 \tag{7}$$

where $\mathbf{A}$ and $\mathbf{B}$ are the parallel and serial Jacobian matrices, respectively, ω is the angular velocity and $\dot{\rho} = [\dot{\rho}_1\ \dot{\rho}_2]^T$ joint velocities [11]. The singularity locus in the worskspace can be written as follows without specifying the design parameters f, r and h [22]:

$$\begin{aligned} &4(C_\beta r + h(f + S_\beta))r(C_\alpha)^2 + (4f^2h^2(C_\beta)^2 - 4f(-S_\alpha r + h(fS_\beta - 1))rC_\beta + \\ &4(h(fS_\beta - 1)S_\alpha - fS_\beta r)r)C_\alpha + 4f((-h^2S_\alpha + rh)(C_\beta)^2 + \\ &h(r(f + S_\beta)S_\alpha + S_\beta h)C_\beta - r(frS_\beta S_\alpha + h)) = 0 \end{aligned} \tag{8}$$

There are three conditions for simplifying and factorizing the singularity equation.

- $h = 0$: $(\sin(\alpha) + \cos(\alpha))(+\sin(\beta) - \cos(\alpha)\cos(\beta)) = 0$
- $f = 0$: $\cos(\alpha)r(h\sin(\alpha) - \cos(\alpha)\cos(\beta)r - \cos(\alpha)\sin(\beta)h) = 0$
- $r = 0$: $\cos(\beta)fh^2(\cos(\alpha)\cos(\beta)f - \sin(\alpha)\cos(\beta) + \sin(\beta)) = 0$

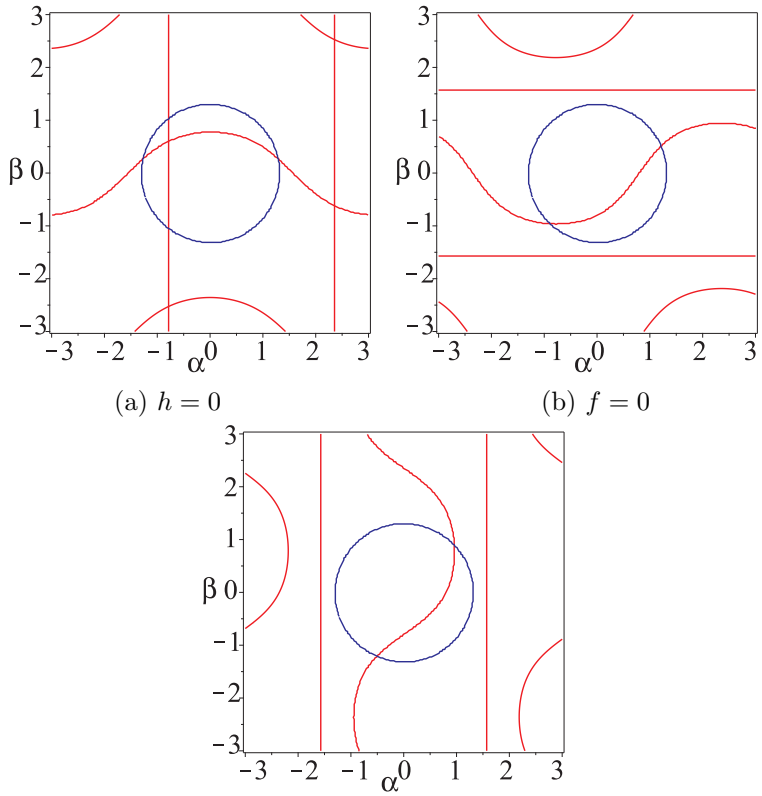

(a) $h = 0$ (b) $f = 0$

(c) $r = 0$

Figure 7: Singularity locus in the workspace of the spherical joint with four aspects where red represents the singularity locus and blue represents the border of the regular workspace shape

When there is simplification of the singularity equations, the DKP admits two of four solutions and each one is located in a given aspect which refers to the maximum singularity free regions in the workspace. These properties are not stable because when a small offset is added, the locus of the singularities changes. The aspects, i.e. the maximum singularity free regions in the workspace are shown in Figure 8 where there are four aspects as shown in Figure 8(a) and (c) and only two in Figure 8(b) [11].

When there is less aspect than solutions to DKP, it means that non-singular assembly mode change trajectories exist, in other words that the mechanism is cuspidal. In order to guarantee the safety of the movements, it is necessary to analyze the uniqueness domains and the behavior around the cusp points.

4.1. Sets of design parameters for the desired workspace

The search for design parameters allowing the inclusion of the desired workspace can be done by optimization or by analyzing the number of intersections between the singularities and the workspace boundary. This is the second solution which is used in this study. It consists in using the CAD of a system formed by the parametric polynomial system of singularities and the equation of the circle, border of the workspace. This system is a function of three design parameters

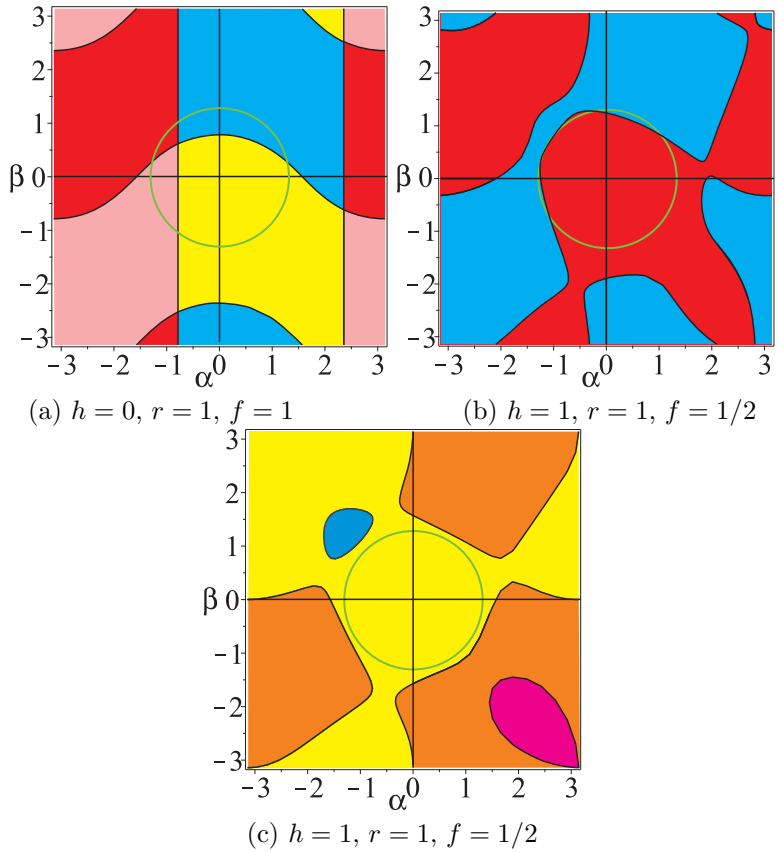

(a) $h = 0$, $r = 1$, $f = 1$ (b) $h = 1$, $r = 1$, $f = 1/2$

(c) $h = 1$, $r = 1$, $f = 1/2$

Figure 8: Singularity locus and aspects in the workspace for three sets of parameters where each color represents a given aspect

and α and β angles.The CAD decomposes the parameter space of the system into cells in which the original system has a constant number of solutions and we retain the components with zero solutions. For each cell obtained, the CAD returns the values of a set of parameters. The following list is obtained by varying by discretization the parameter f to have a 2D view of the other parameters h and r. Table 1 is a list of solutions by a set of parameters solutions of each cell for $r = 1$ and Figure 9 depicts the singularity locus of each set of parameters.

If the design parameters make it possible to obtain the desired workspace, there are two singularity typologies. Two examples are now presented, one where the equation of factor singularities factorizes and the other where we cannot, to divide the workspace into four aspects. Figure 10(a) is the set of design parameters for $f = 0$. This set include $h = 0$ but also small value of h with respect to r. Figure 10(b) and (c) are the set of solutions for $f = 1$ and $f = 2$, respectively.

4.2. Example 1: $h = 0$, $r = 1$ and $f = 1/10$

For $h = 0$, $r = 1$ and $f = 1/10$, the singularity locus is defined as

$$(10\cos(\alpha)\cos(\beta) - \sin(\beta))(\sin(\alpha) + 10\cos(\alpha)) = 0 \tag{9}$$

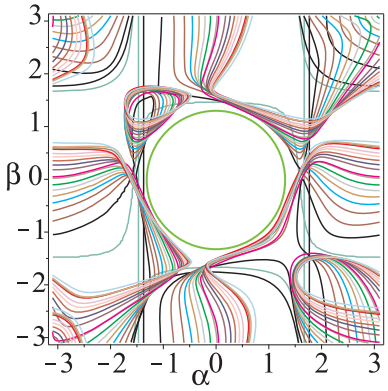

Figure 9: Singularity locus from the parameters defined in Table 1 where the blue curve is the boundary of the prescribed workspace

h	0	0	0.233	0.408	0.549	0.648	0.735	0.818	0.898	1.038
f	0.1	0.2	0.3	0.4	0.5	0.6	0.7	0.8	0.9	1
h	1	1.204	1.341	1.478	1.616	1.753	2	2	2	2.308
f	1.1	1.2	1.3	1.4	1.5	1.6	1.7	1.8	1.9	2

Table 1: Set of parameters solutions of each cell for $r = 1$ obtained by the CAD

Figure 11 depicts the workspace and the joint space as well as the boundary of the prescribed workspace. As there is only two (area in green) or four real solutions (area in red) to the DKP and the singularity can be factorized, there is no cusp point in the joint space. As the boundary of the prescribed workspace is on the boundary of the aspect, its image in the joint space is also on the boundary. This solution does not yield a safety problem during the trajectory planning.

4.3. Example 2: $h = r = f = 1$

For $h = r = f = 1$, the singularity locus is defined as

$$\begin{aligned} & 2(C_\beta + S_\beta + 1)C_\alpha^2 + (2C_\beta^2 + (-2S_\beta + 2S_\alpha + 2)C_\beta + (-2S_\alpha + 2)C_\beta^2 \\ + \quad & (2S_\beta - 2)S_\alpha - 2S_\beta)C_\alpha + ((2S_\beta + 2)S_\alpha + 2S_\beta)C_\beta - 2S_\alpha S_\beta = 2 \end{aligned} \tag{10}$$

Figure 12(b) depicts the joint space where the DKP admits either two real solutions, in green, four real solutions, in red and six real solutions, in yellow. Eight cusps exist (i) C_1, C_2 and C_3 are between the two- and four-solution regions solutions to the DKP, and (ii) C_4, C_5, C_6, C_7 and C_8 are between the four- and six-solution regions. The workspace devided into four aspects (regions in orange, pink, blue and yellow).

The analysis of the image of the boundary of the prescribed workspace (Figure 12(a)) in the joint space has been studied in [22]. This curve surrounds 3 cusp points C_4, C_5 and C_6 (Figure 12(b)). When a prescribed workspace is inscribed in a single aspect, it does not lead to the conclusion that the trajectories that the robot will make will be in a single domain of uniqueness, i.e. there is no non-singular assembly mode changing.

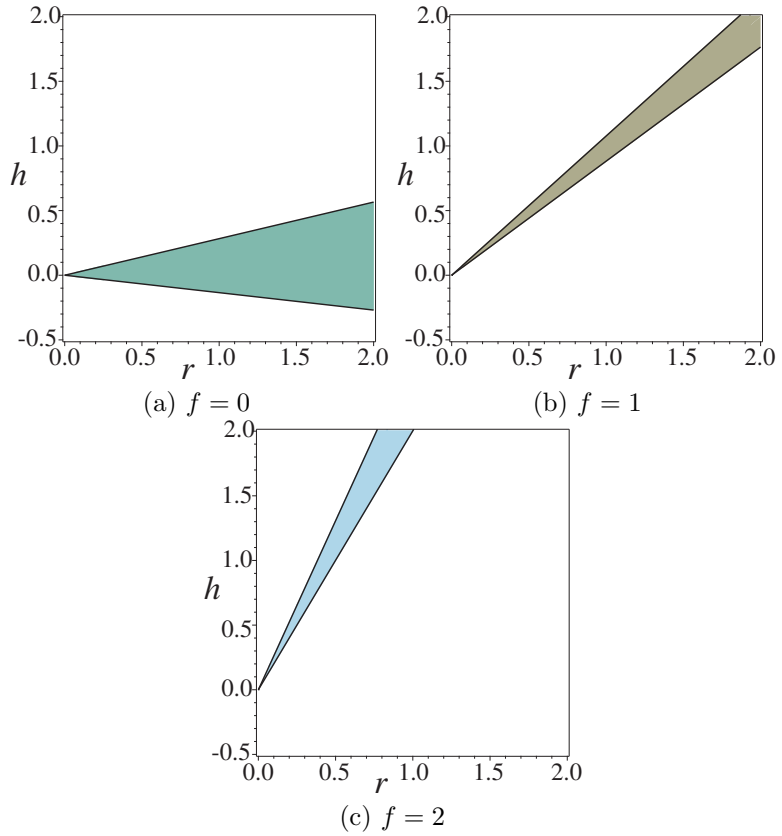

Figure 10: Set of solutions obtained by CAD

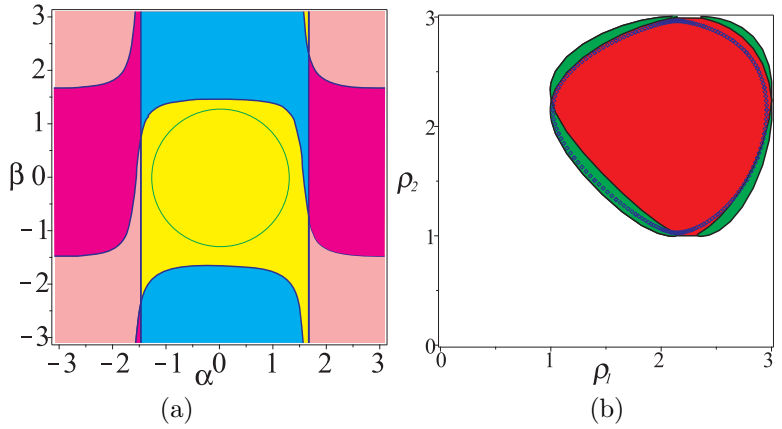

Figure 11: Workspace (a) and joint space (b) without any cusps points with the boundary of the prescribed workspace and its image in the joint space for $h = 0$, $r = 1$ and $f = 1/10$

Either point Q belonging to the workspace boundary whose image in the workspace is located in a region where DKP admits six solutions, called P_i. We realize a loop that includes the cusp point C_6 (Figure 13(a)).

The images of this trajectory shown in Figure 13(b) in the workspace are lo-

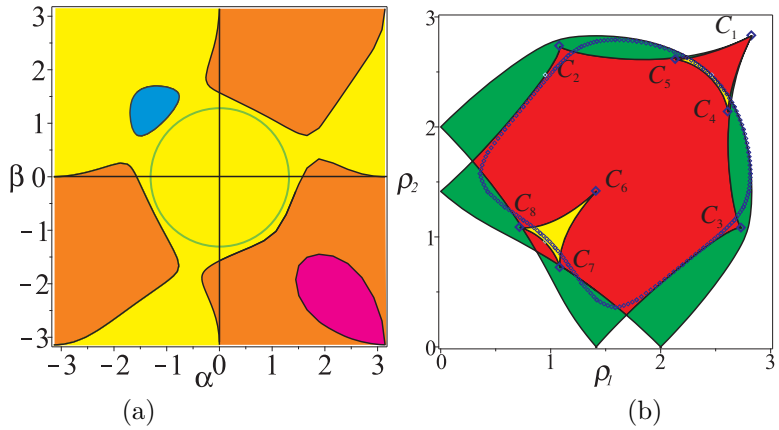

Figure 12: Workspace (a) and joint space (b) with height cusps points with the boundary of the prescribed workspace and its image in the joint space for $h = r = f = 1$

cated in basic regions depicted in yellow and blue regions where $\det(\mathbf{A}) > 0$ and in basic region depicted in red and green where $\det(\mathbf{A}) < 0$. In Figure 13(b), we can observe from any stating point P_i (i) two singular trajectories between two aspects ($P_4 - P_6$ and $P_5 - P_6$) and meet singular positions in S_1 and S_2, respectively, (ii) one non-singular changing trajectory in the same aspect ($P_4 - P_5$), and (iii) three loops in the workspace located in the same aspect ($P_1 - P_1$, $P_2 - P_2$, $P_3 - P_3$). Only the trajectory ($P_1 - P_1$) is located in the regular workspace shape. We can therefore conclude that even if this trajectory surrounds a cusp point in the joint space, it is not a non-singular trajectory in a changing assembly mode.

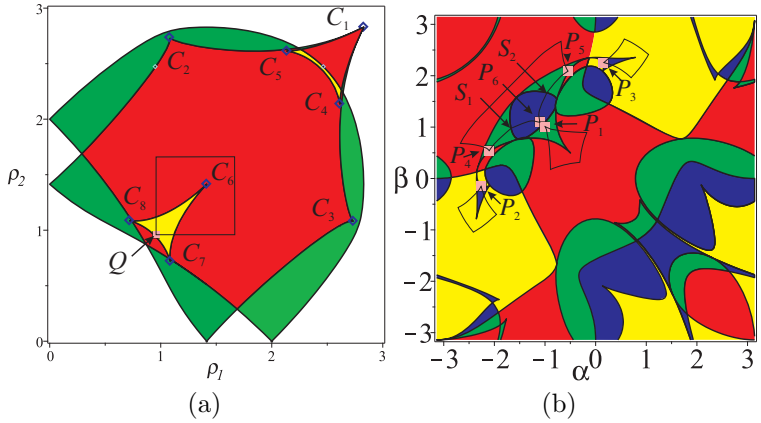

Figure 13: Trajectory that encircles a cusp point in the joint space and its image in the workspace

4.4. Discussions

The study of mechanism in the design parameter space allows a better understanding of the architecture and the working of the 2-PUS-U robot. There are three design parameters (namely f, r and h) associated with the proposed

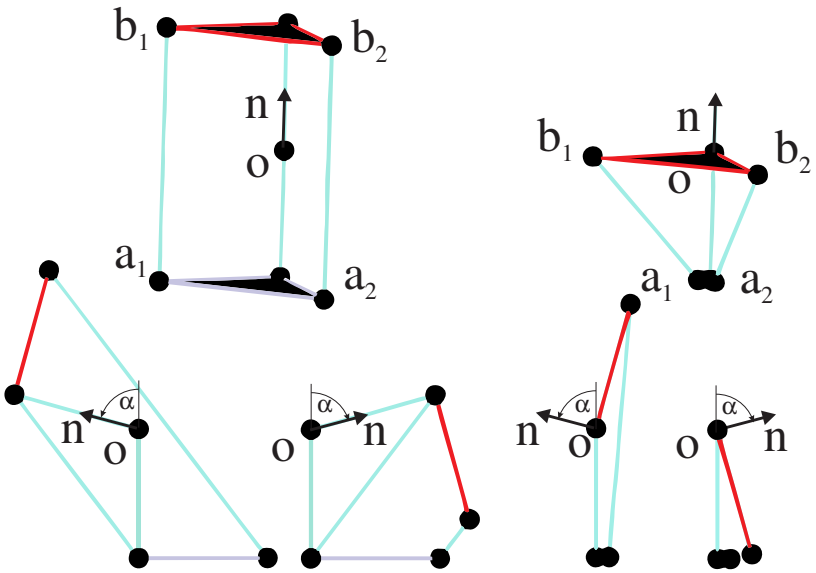

(a) $h = r = f = 1$ (b) $h = 0$, $r = 1$, $f = 1/10$

Figure 14: Graphic rendering of the two cases under study in the home pose and for $\alpha = \pm 75°$ with the mobile platform in red and $\mathbf{n}$ the normal to the mobile platform

robot. The singularity equation is analysed, based on the three conditions ($f = 0$, $r = 0$ and $h = 0$), which further helps to simplify and factorize the singularity equations which is shown in Figure 7. It is shown that robot will have non-singular assembly mode changing trajectories i.e. it will be cuspidal if it has less aspect than the solutions to the DKP. The analysis of uniqueness domains and the behavior around the cusp points infers the safe movement of the robot. The selection of design parameters for the desired workspace is obtained by analyzing the number of intersections between the singularities and the workspace boundary. The CAD algorithm is used to compute and visualize the two dimensional surface in $h - r$ plane by varying the design parameter f value. More homogeneous sets of parameters exist but make the robot cuspidal with possible dangers when generating trajectories. It has been shown that in reported case, the part of the workspace studied does not lead to non-singular assembly mode changes. However, this does not allow us to infer this result for all design parameters.

Figure 14 depicts the graphic rendering of the robot with the same scaling for the two examples studied. In the "home" position, for the first example, the design is more compact than the second example as the width of the first case is twice the width of the second case while its height is half the height of the second case. However, this selection of design parameters is not generic and it is impossible to design the robot as one of the design parameter equal to zero. At the maximum tilt rotations, it is necessary to take into account the interference problems between the UPS leg actuators and the central link formed by the universal joint.

5. Conclusions

Based on the analysis of the surgeon's needs of otologic operations, the definition of a regular workspace shape was defined. This property allow the robot to be adapted to the human anatomy of a large part of the population. A 2UPS-U spherical parallel robot was presented and its kinematic equations were formulated. The properties of this robot were studied in the design parameter space. Several simplifications have been proposed which allow a factorization of the singularity locus when one of the parameters is equal to zero. The workspace can be divided into two or four aspects. A CAD is used to characterize the sets of design parameters where there is no intersection between the singularity curves and the regular workspace shape. From this set of possible solutions, two examples are presented, a non cuspidal robot and a cuspidal robot. Their properties were illustrated in the workspace and in the joint space. In both cases, the prescribed workspace is safe because the robot does not change the assembly mode. Further research will be conducted in order to verify the collision between the legs and the joint limits of the passive joints and to use a kinetostatic criteria to select the optimized design parameters of the mechanism for the surgery application.

References

[1] Cohen, M.S., Basonbul, R.A., Barber, S.R., Kozin, E.D., Rivas, A.C. and Lee, D.J. Development and validation of an endoscopic ear surgery classification system. The Laryngoscope, 128(4), pp.967-970 (2018).

[2] Iannella, G., Marcotullio, D., Re, M., Manno, A., Pasquariello, B., Angeletti, D., Falasca, V. and Magliulo, G.. Endoscopic vs microscopic approach in stapes surgery: advantages in the middle ear structures visualization and trainee's point of view. The journal of international advanced otology, 13(1), p.14 (2017).

[3] Dahroug, B., Tamadazte, B., Weber, S., Tavernier, L. and Andreff, N. Review on otological robotic systems: Toward microrobot-assisted cholesteatoma surgery. IEEE reviews in biomedical engineering, 11, pp.125-142 (2018).

[4] Schena, B., Robotic manipulator with remote center of motion and compact drive, Patent WO 2008/157225 (2007).

[5] Rosen, J., Brown J.D., Chang, L., Barreca, M., Sinanan, M., Hannaford, B., The Blue-DRAGON - a system for measuring the kinematics and dynamics of minimally invasive surgical tools in-vivo, In: Proc. IEEE International Conference on Robotics and Automation (2002).

[6] Gosselin, C., Hamel, J.-F., The agile eye: a high-performance three-degree-of-freedom camera-orienting device. In: Proc. IEEE international conference on robotics and automation, pp. 781–786 (1994).

[7] Cheng H.H., Real-time manipulation of a hybrid serial-and-parallel driven redundant industrial manipulator. ASME J. of Dynamic Systems, Measurement and Control, 116(4), pp. 687–701 (1994).

[8] Agrawal S.K., Desmier G., Li S., Fabrication and analysis of a novel 3 dof parallel wrist mechanism, ASME J. of Mechanical Design, 117(2), pp. 343–345 (1995).

[9] Caron, F., Analyse et développement d'un manipulateur parallèle sphérique à deux degrés de liberté pour l'orientation d'une caméra, M.Sc., Université Laval, Québec, August (1997).

[10] Karouia M. and Hervè J.M. A three-dof tripod for generating spherical motion, In ARK, pp.395–402, Piran, 25-29 June (2000).

[11] Chablat, D., and Wenger P., Working modes and aspects in fully parallel manipulators; Proceedings, 1998 IEEE International Conference on Robotics and Automation, Vol. 3 (1998).

[12] Bonev, I. A., Chablat D., and Wenger P., Working and assembly modes of the Agile Eye, Proceedings 2006 IEEE International Conference on Robotics and Automation (2006).

[13] Kumar, S., Nayak, A., Peters, H., Schulz, C., Müller, A., Kinematic analysis of a novel parallel 2SPRR+ 1U ankle mechanism in humanoid robot, International Symposium on Advances in Robot Kinematics. Springer, Cham (2018).

[14] Chablat D., Wenger P., Séparation des solutions aux modèles géométriques direct et inverse pour les manipulateurs pleinement parallèles, Mechanism and Machine Theory, Vol 36/6, pp. 763–783, (2001).

[15] Wenger Ph., Chablat D., Definition Sets for the Direct Kinematics of Parallel Manipulators, 8th International Conference in Advanced Robotics, pp. 859–864 (1997).

[16] Jha, R., Chablat, D., Baron, L., Rouillier, F., Moroz, G., Workspace, joint space and singularities of a family of delta-like robot, Mechanism and Machine Theory, 127, pp. 73–95, (2018).

[17] Chablat, D., Moroz, G., Rouillier, F., Wenger, P., Using Maple to analyse parallel robots. In Maple Conference 2019, October, (2019).

[18] Michel, G., Haribhau Salunkhe, D., Chablat, D. and Bordure, P., A New RCM Mechanism for an Ear and Facial Surgical Application, Proceedings Advances in Service and Industrial Robotics, Springer International Publishing, Cham, pp. 408–418, 2020.

[19] Bonev, I. A., D. Zlatanov, and C. M. Gosselin. "Advantages of the modified Euler angles in the design and control of PKMs." 2002 Parallel Kinematic Machines International Conference (2002).

[20] Chablat, D., Wenger, P., Majou, F., and Merlet, J. P."An interval analysis based study for the design and the comparison of three-degrees-of-freedom parallel kinematic machines". The International Journal of Robotics Research, 23(6), 615-624, 2004.

[21] Chablat, D., Michel, G., Bordure, P. (2019), Dispositif d'aide à la chirurgie, PCT/EP2020/076353, European Patent.

[22] Chablat, D., Michel, G., Bordure, P., Jha, R., & Venkateswaran, S. (2020, September). Joint space and workspace analysis of a 2-DOF Spherical Parallel Mechanism. In European Conference on Mechanism Science (pp. 181-188). Springer, Cham.